Gene Expression of Disease-related Genes in Alzheimer's Disease is Impaired by Tau Aggregation

G. Siano [1], M. Varisco [1†], A. Scarlatti [1], M. C. Caiazza [1‡], K. Dunville [1], F. Cremisi [1], M. Costa [2], L. Pancrazi [2], C. Di Primio [1,2*] and A. Cattaneo [1*]

1 - *Laboratorio di Biologia BIO@SNS,* Scuola Normale Superiore, Pisa, Italy
2 - *Istituto di Neuroscienze,* CNR, Pisa, Italy

Correspondence to C. Di Primio and A. Cattaneo: Laboratorio di Biologia BIO@SNS, Scuola Normale Superiore, Pisa, Italy. *cristina.diprimio@sns.it* (C. Di Primio), *antonino.cattaneo@sns.it* (A. Cattaneo)
https://doi.org/10.1016/j.jmb.2020.10.009
Edited by Louise C. Serpell

Abstract

Neuronal hyperexcitability linked to an increase in glutamate signalling is a peculiar trait of the early stages of Alzheimer's disease (AD) and tauopathies, however, a progressive reduction in glutamate release follows in advanced stages. We recently reported that in the early phases of the neurodegenerative process, soluble, non-aggregated Tau accumulates in the nucleus and modulates the expression of disease-relevant genes directly involved in glutamatergic transmission, thus establishing a link between Tau instability and altered neurotransmission. Here we report that while the nuclear translocation of Tau in cultured cells is not impaired by its own aggregation, the nuclear amyloid inclusions of aggregated Tau abolish Tau-dependent increased expression of the glutamate transporter. Remarkably, we observed that in the prefrontal cortex (PFC) of AD patient brain, the glutamate transporter is upregulated at early stages and is downregulated at late stages. The Gene Set Enrichment Analysis indicates that the modulation of Tau-dependent gene expression along the disease progression can be extended to all protein pathways of the glutamatergic synapse. Together, this evidence links the altered glutamatergic function in the PFC during AD progression to the newly discovered function of nuclear Tau.

Introduction

Amyloidogenic aggregates, synaptic loss and neuronal cell death leading to severe memory deficits are characteristic of Alzheimer's disease (AD) and tauopathies. Several altered functions, such as axonal transport, microtubules (MT) destabilization, oxidative stress and altered neurotransmission, likely converge upon the onset and progression of the pathology though the exact molecular mechanisms involved are still elusive.[1–4]

Longitudinal studies on patients and models indicate increased neuronal activity in concomitance with higher release of glutamate neurotransmitter at early stages.[5–9] This alteration leads to neuronal hyperexcitability and activates cellular pathways related to synaptic dysfunction and apoptosis, triggering the pathological cascade.[10–12] However, at late stages, this phenomenon is reversed toward a reduction in glutamate release, a progressive impairment in neuronal activity, and a volumetric reduction of several brain areas linked to cell death and memory loss.[13]

Despite altered cellular neurotransmitter response mediated by amyloid beta (Aβ) and Tau, the mechanisms involved in the pathological

modulation of glutamate release and neurotransmission are still debated.[9,14,15]

At early stages, Tau destabilization from microtubules is associated with altered axonal transport and dendritic glutamate receptor dysregulation, thus affecting synaptic transmission.[2,16–20] In tauopathic human brains and in pathological Tau models, early hyperexcitability is associated with a higher probability of seizures.[21,22] The close connection between Tau and hyperexcitability is also evident in epilepsy models wherein the reduction of Tau leads to a reduction in seizures.[23,24]

While Tau destabilization and hyperexcitability are observed at the onset of AD, the role of Tau aggregation on neuronal activity at late stages is still unclear. In AD brains, the neurofibrillary tangles (NFTs) are detectable in several regions characterized by alterations in synaptic plasticity and transmission, synaptic loss, and neuronal cell death.[14,25,26] Previous studies indicate that Tau aggregation affects the transport and release of vesicles at the synapse, altering neurotransmission.[13,27,28] Moreover, electrophysiological experiments on mouse brains treated with Tau aggregates showed a reduction in neurotransmission as well as synaptic plasticity.[14] This evidence suggests a causal link between the Tau-solubility state and the altered neurotransmission. By mimicking the early events occurring in AD on the cellular level, we previously demonstrated that Tau detachment from microtubules boosts its nuclear translocation and that nuclear Tau triggers an increase in both the vesicular glutamate transporter 1 (VGluT1) and NMDAR expression. Remarkably, this Tau-dependent specific modulation of gene expression induces neuronal hyperexcitability in neurons post-synaptic to glutamatergic neurons.[29]

Here we study the effect of Tau-aggregation on Tau-dependent gene expression, focusing on the glutamate release pathway. We report that Tau aggregates are also found in the neuronal nuclear compartment and that, concomitantly, VGluT1 expression decreases, indicating that aggregation causes the loss of Tau-dependent gene expression. Moreover, we analysed the longitudinal transcriptome of the prefrontal cortex (PFC) from AD patients and found that VGluT1 levels increased in early stages and decreased during later stages, shown by a bell-shaped modulation overlapping with Tau destabilization at early stages and then with Tau aggregation at late stages. Additionally, we observed changes in VGluT1 expression which recapitulate glutamate release pathway events in the prefrontal cortex of AD patients.

Altogether, this evidence suggests the role of Tau aggregates on disease-related gene expression as well as on resultant synaptic transmission alterations observed during AD progression. Our findings introduce a novel pathological mechanism that can be targeted to prevent the progression of neurodegeneration.

Results

Tau aggregates into the nucleus

We previously reported Tau nuclear translocation and accumulation because of either Tau overexpression or after Tau detachment from MTs. In these conditions, nuclear Tau increased the expression of VGluT1, a disease-relevant gene directly involved in glutamatergic synaptic transmission.[29] To investigate whether Tau nuclear translocation is altered during the aggregation process, we expressed the 0N4R Tau isoform harbouring the P301S mutation in HT22 hippocampal immortalized neurons and we induced its aggregation with synthetic Tau seeds, as previously described.[30] The nuclear compartment (NF = nuclear fraction) was isolated by subcellular fractionation and analysed by western blot. We observed that in Tau expressing cells its nuclear accumulation increased, as expected[29] (Figure 1(a) and (b)); however, this effect is not altered by aggregation. Indeed, nuclear Tau accumulation in seed-treated cells is comparable to that in untreated cells, indicating that the aggregation process does not interfere with the nuclear translocation of Tau. Moreover, by qPCR we verified that the expression of Tau is not altered by seed treatment (Supplementary figure 1(A)). To investigate whether Tau monomers could aggregate in the nuclear compartment we performed imaging experiments in cells expressing Tau fused to YFP. Cells have been treated with unlabelled seeds and, as shown in Figure 1(c), fluorescent inclusions become detectable in both the cytoplasm and the nucleus (Figure 1(c)). To verify that nuclear fluorescent spots correspond to amyloidogenic proteopathic aggregates, the K114 staining for β-sheet amyloid fibrils was performed. Remarkably, Tau inclusions are positive to K114 also in the nuclear compartment, demonstrating that nuclear aggregates share structural characteristics with pathological Tau fibrils (Figure 1 (d), Suppl. Figure 1(B)–(D)).

Having established that Tau amyloid aggregates are detectable in the nucleus, we investigated whether nuclear Tau molecules undergo aggregation as well as cytoplasmic ones. To this aim, we expressed the Tau^{NLS}-YFP, whose localization is mainly restricted in the nuclear compartment due to the nuclear localization signal (NLS). We treated cells with Tau seeds and small fluorescent inclusions appeared in the nucleus 48 h later (Figure 1(e)).

To further investigate whether nuclear Tau undergoes aggregation or if Tau aggregates translocate to the nucleus, we transiently expressed Tau^{NLS}-YFP and a Tau-CFP that is ubiquitously expressed. The two constructs were
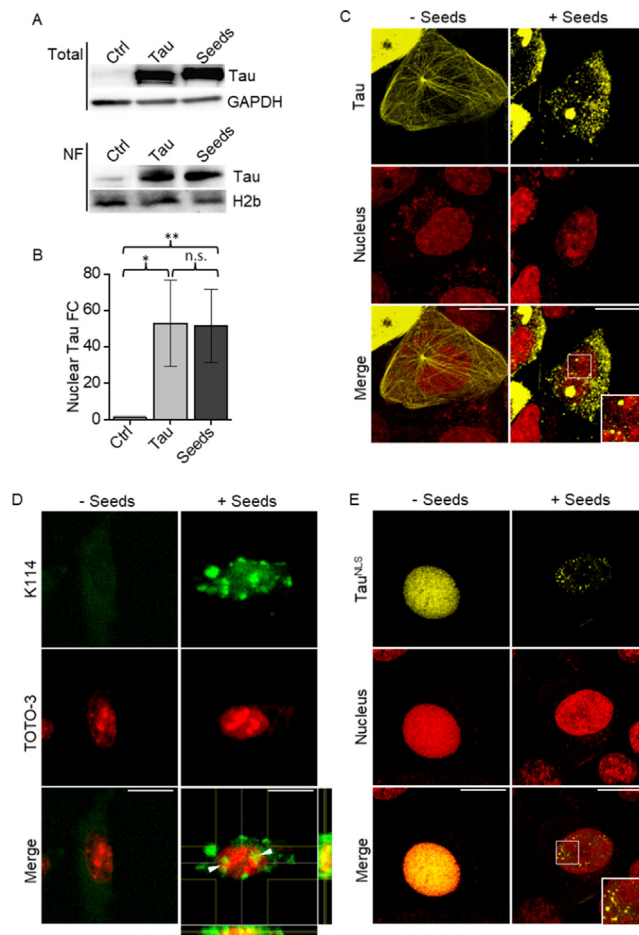
Figure 1. Nuclear Tau accumulation is not altered by aggregation and aggregates are detected into the nucleus. (A) The total extract and the nuclear fraction (NF) of HT22 cells, expressing the Tau 0N4R bearing the P301S mutation, treated or untreated with Tau seeds was analyzed by WB to quantify the enrichment in Tau signal. Control cells are transfected with empty vector. (B) Quantification of A. (Kruskal-Wallis ANOVA and Mann-Whitney test; ** $p < 0.01$; * $p < 0.05$). Control cells are transfected with empty vector. FC = Fold Change; $N = 5$. (C) Immunofluorescence of YFP-Tau^{P301S} expressing cells treated with Tau seeds (seeds) or untreated; Tau (Yellow), Nuclear ID (red). (D) Nuclear K114 immunostaining of cells treated with Tau seeds or untreated; K114 (green), TOTO-3 (red). White arrows indicate nuclear spots in the 3D section. (E) Immunofluorescence of YFP-Tau^{P301S}-NLS expressing cells treated with Tau seeds or untreated; Tau (Yellow), Nuclear ID (red). Images are reported as Z-stacks; Scale bar: 10 μM.

co-expressed and cells were treated with seeds. We observed in the cytoplasm the formation of CFP positive aggregates without the contribution of Tau^{NLS}-YFP, as expected. Conversely, in the nucleus we observed aggregates containing both Tau^{NLS}-YFP and Tau-CFP as well as aggregates containing only Tau^{NLS}-YFP. Furthermore, no nuclear aggregates containing only Tau-CFP were detected (Figure 2). These results suggest that nuclear aggregates mainly form in the nucleus.

Aggregation inhibits Tau-dependent VGluT1 expression

To investigate the impact of aggregation on Tau-dependent gene expression, we measured the

levels of VGluT1 in cells expressing aggregated Tau. Previously, we demonstrated that P301L mutation does not increase VGluT1 expression with respect to control cells. Here, employing P301S mutation to induce aggregation, we first checked whether the P301S mutation also alters VGluT1 expression. As reported in Suppl. Figure 1, we observed that it behaves differently from P301L Tau, preserving the Tau-dependent modulation on VGluT1.

In Figure 3(a) and (b), the expression of VGluT1 in Tau expressing cells is increased as expected, but upon aggregation, returns to the control level. This modulation has also been confirmed at mRNA level by qPCR (Figure 3(c)). To demonstrate that this effect is triggered by
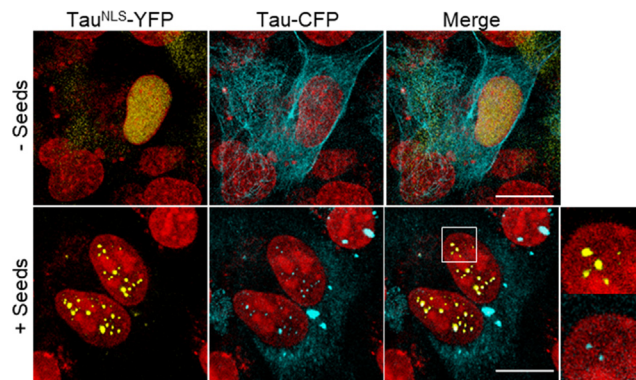
Figure 2. Aggregation of nuclear Tau occurs in the nuclear compartment. Confocal imaging of HT22 cells transiently expressing Tau^{NLS}-YFP (0N4RTauP301S-NLS-YFP) and Tau-CFP (0N4RTauP301S-CFP) and treated or untreated with seeds. Magnification in the merge panel to visualize nuclear aggregates. Tau^{NLS}-YFP (yellow); Tau-CFP (cyan); NuclearID (red). Images are reported as Z-stacks; Scale bar: 10 μM.
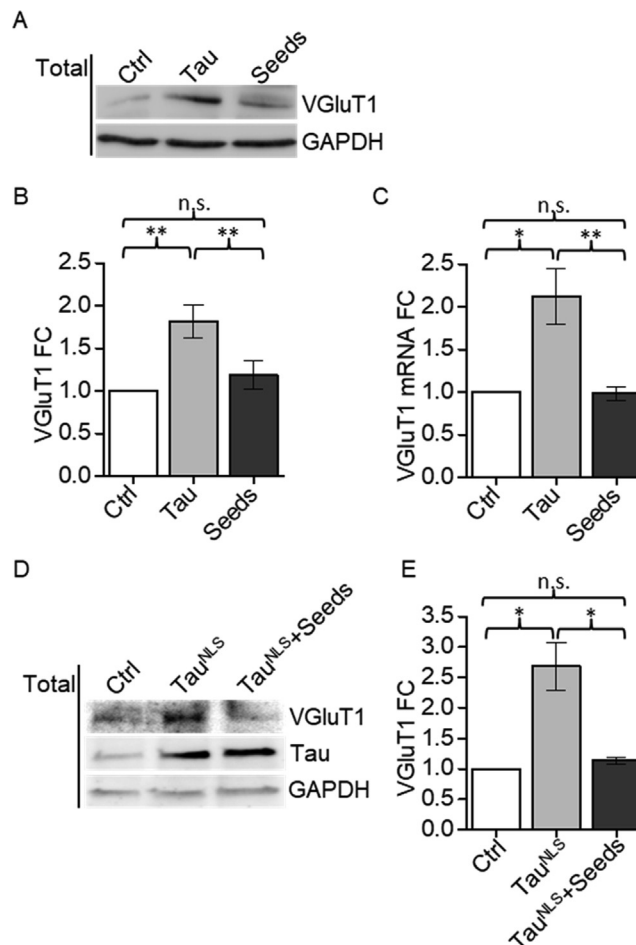

Figure 3. Aggregation inhibits Tau-dependent expression of VGluT1. (A) The total lysate of cells treated or untreated with Tau seeds was analysed by WB to quantify the VGluT1 signal. (B) Quantification of VGluT1 protein signal in A. (Kruskal-Wallis ANOVA and Mann-Whitney test; **$p < 0.01$). $N = 5$. (C) VGluT1 mRNA quantification by qPCR in treated and untreated cells (Mann – Whitney test; **$p < 0.01$). $N = 4$. (D) The total lysate of cells expressing Tau^{NLS} (0N4RTau-P301S-NLS) treated or untreated with Tau seeds was analysed by WB to quantify the VGluT1 signal. (E) Quantification of VGluT1 protein signal in D. $N = 4$. (Kruskal-Wallis ANOVA and Mann-Whitney test; *$p < 0.05$). FC = Fold Change.

nuclear Tau, we performed the same experiment in cells expressing Tau[NLS] and we observed an increase of VGluT1 expression by WB, as reported in Figure 3(d) and (e). On the contrary, the expression of VGluT1 returns to baseline upon aggregation induction, indicating that nuclear aggregation impairs the Tau-dependent VGluT1 expression.

At the cellular level, this indicates that Tau-dependent modulation of VGluT1 might roughly follow a bell-shaped longitudinal distribution wherein VGluT1 increase is caused by soluble Tau monomers accumulated in the nucleus and is followed by a strong decrease of VGluT1 expression in the presence of Tau aggregates.

To ask whether this mechanism is also conserved in neurons, we performed the same experiment on cortical neurons derived from mouse embryonic stem cells (ESCs). Untreated and seed-treated cells were subjected to immunofluorescence acquisition to quantify VGluT1 expression. Accordingly, VGluT1 expression increased in Tau expressing cells, while it decreased in aggregation conditions (Supplementary Figure 2(A) and (B)).

Tau-dependent modulation of VGluT1 in the prefrontal cortex of AD patients

To investigate whether this *in vitro* evidence could resemble the *in vivo* pathological condition, we performed a comparative transcriptome analysis of the prefrontal cortex of AD patients derived from the GSE84422 public dataset.[31] The dataset allows separation of patients at different Braak stages (BS) and we plotted VGluT1 as a function of the disease progression. As reported in Figure 4(A), VGluT1 expression in the prefrontal cortex of AD patients is upregulated at early stages (BS3-4) and downregulates at the late stage (BS6). To evaluate how glutamatergic function is altered in the PFC along pathology progression, we identified pathways related to the glutamatergic synapse by a gene set enrichment analysis (GSEA) at each Braak stage. KEGG pathways related to glutamatergic synaptic activity in the prefrontal cortex have been isolated (Figure 4(B)). Four gene pathways (glutamatergic synapse, Long-term depression, Long-term potentiation, synaptic vesicle cycle) share the same trend: overrepresented at Braak stages 3 and 4, but not significantly modulated at Braak stage 6. This indicates that there is a strong functional alteration specifically during early stages. We also checked unrelated gene sets affected *versus* unaffected at Braak stage 3-4-6 and a short list is reported in Supplementary Table 1. We found that protein export, processing, and degradation pathways undergo a persistent modulation in the diseased brain as expected. On the contrary, basic metabolic and biosynthetic pathways tend to not be altered throughout disease progression.

Altogether, these results clearly indicate that glutamatergic function can be described by a bell-shaped curve during AD progression in the prefrontal cortex of human patients, similarly to the expression of Tau-induced glutamate transporter at the cellular level. Our results suggest that Tau aggregation may have an important role in the dysfunction of the glutamatergic function, in addition to other pathological mechanisms.

Discussion

We previously demonstrated that Tau, a well-established MT-associated protein, translocates to the nucleus, where it modulates the expression of genes specifically involved in glutamatergic synaptic transmission. This role might partially account for the strong change in synaptic transmission commonly occurring during Tau pathology progression. Indeed, in tauopathy mouse models and in AD human patients, glutamate release increased in the pre-symptomatic phase correlates with toxic circuit hyperexcitability while later this is followed by an impairment in glutamate release.[7,13,16,27,32–35] According to this evidence, when Tau destabilizes from MTs but does not aggregate, nuclear translocation of Tau increases and nuclear Tau molecules drive the expression of a set of genes involved in glutamatergic transmission, like VGluT1 and NMDA receptor subunits, thereby increasing the synaptic activity of primary cultured neurons.[29]

Here we reported that in later phases of the disease, Tau-dependent VGluT1 expression downregulates to basal levels in the presence of proteopathic aggregates. Interestingly, while the aggregation event does not alter the amount of Tau in the nuclear compartment, we observed nuclear inclusions of aggregated Tau. Previous evidence indicated the presence of aggregates in the nucleus in particular experimental conditions but also in human AD brains. Tau PHF strands within the AD brain nuclei was first reported in Metuzals *et al.*[36]; later the structure of Tau rod-like nuclear deposits has been described in both AD and Huntington disease.[37] Benhelli-Mokrani *et al.* reported the presence of pathological prefibrillar oligomerized forms of Tau protein in the cytoplasm and in the nuclei of THY-Tau22 CA1 neurons after heat shock treatment.[38] Sanders *et al.* generated Tau strains that induce different pathologies *in vivo* depending on distinct amyloid conformations. Interestingly, one of these strain is characterized by the presence of Tau nuclear speckles both in cell lines and in three generations of inoculated transgenic mice.[39] The role of Tau aggregates in the nucleus is still obscure though recently the repressive role of Tau oligomers has been suggested by measuring the expression rates of Tau-interacting genes in brain extracts from WT
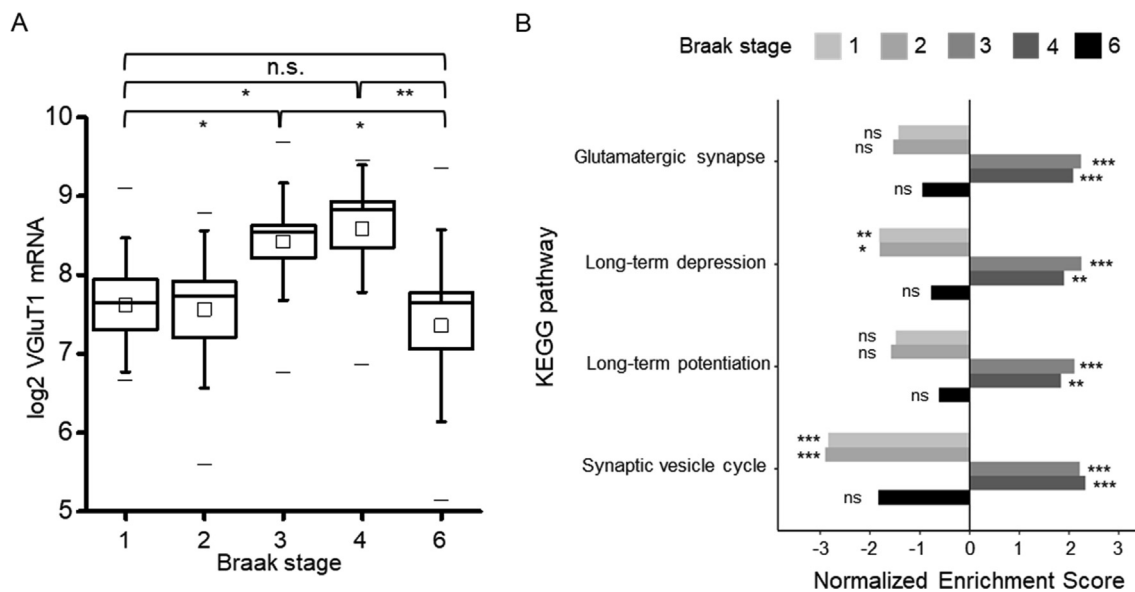
Figure 4. VGluT1 and the glutamatergic synapse are altered in the brain of AD patients at intermediate, but not at late disease stages. (A) Boxplot of VGluT1 expression in the prefrontal cortex of AD patients classified by Braak stage. Stage 1 $N = 7$, stage 2 $N = 8$, stage 3 $N = 13$, stage 4 $N = 11$, stage 6 $N = 16$. Stage 5 is not represented due to the absence of samples from stage 5 patients. Kruskal-Wallis ANOVA; $^*p < 0.05$; $^*p < 0.01$. (B) Enrichment of KEGG pathways related to glutamatergic synaptic activity in the prefrontal cortex by GSEA. Only significantly deregulated pathways (FDR < 0.05) are shown. Synaptic pathways are upregulated at Braak stage 3 and 4, but are not significantly modulated at Braak stage 6.

and KO Tau mice. Interestingly, the repression was predominantly observed under heat shock conditions in correlation with the increased presence of Tau oligomers within neuronal nuclear compartment.[38]

In this study we employed the Tau-P301S mutant as a reliable and widely used strategy to induce Tau aggregation by initial assessment of this mutant's ability to modulate VGluT1 expression. Interestingly, unlike the P301L mutation, P301S preserved the ability to modulate the disease-related gene underlying the known observation by other authors that the two mutations have different impacts on the pathology.[40,41] Our result could be mechanistically related to these differences in the pathological impact of P301 mutations to L or to S, and especially on gene expression modulation.

Here we report that Tau aggregates are detectable in the nuclear compartment. Moreover, we demonstrated that aggregation can occur in the nucleus without the contribution of cytoplasmic Tau.

We report the appearance of Tau aggregates in the nucleus and the concomitant loss of function, in terms of Tau-dependent VGluT1 expression. This confirms previous observations and demonstrates that Tau aggregates impact also on the expression of disease-related genes such as VGluT1. Remarkably, we demonstrated that nuclear aggregates impair the Tau-dependent

modulation of VGluT1 gene suggesting that aggregated Tau is unable to interact with DNA regions or with nuclear cofactors mediating gene expression. Aggregates might physically prevent transcription or might recruit factors involved in gene expression. Nuclear aggregates component analysis could reveal the molecular basis of this novel repressive mechanism.

This *in vitro* evidence strongly recapitulates what happens in human brains when compared to the longitudinal transcriptome of the prefrontal cortex (PFC) of AD patients. The PFC is a hub region responsible for linking functionally specialized regions whose ability to process information is increasingly affected with AD progression. Clinical studies on human brains revealed that Tau aggregation in the PFC occurs in late stages, however, pathological Tau hallmarks, like Tau hyperphosphorylation and delocalization, are detectable earlier. Remarkably, the spreading of Tau pathology in the PFC might be caused by its functional connections with hippocampal and cortical regions.[25,42–44] The clinical and pre-clinical connectome of the hippocampal–PFC circuit in the disease progression demonstrated the effect of the initial deposition of NFTs on distal brain regions at early stages of the pathology.[42–44] Our analysis highlights that VGluT1 expression is significantly upregulated at early stages in the PFC of AD brains (BS 3-4) but downregulates in the late stage (BS 6).

Despite the limited number of human samples available, this bell-shaped modulation is significant, confirming a similar trend observed in our cellular model and further supporting the role of Tau-dependent gene expression modulation alongside disease progression.

The GSEA analysis performed provides pathways that depend on significant alterations of genes functionally categorized in that pathway, not necessarily all genes in the same direction. In this analysis, four gene pathways related to the glutamatergic synapse along the pathology progression (glutamatergic synapse, Long-term depression, Long-term potentiation, synaptic vesicle cycle) share a trend: they are altered at Braak stage 3 and 4 but are not significantly modulated at Braak stage 6. This evidence clearly indicates that the altered glutamatergic function during AD progression in the PFC is strongly correlated to the glutamate transporter expression at cellular level.

In light of these findings, it could be useful to carefully evaluate memantine as a treatment option for AD and to reconsider the clinical stage of patients to be treated. Memantine is a NMDAR antagonist and was approved by FDA as a therapeutic drug in moderate to severe AD in 2003.[45] Our results suggest that the effectiveness of memantine might be greater at very early stages, when the glutamatergic transmission is abnormally increased, though may be detrimental as the disease progresses along the bell shaped curve. This study suggests that nuclear Tau has peculiar functions still unexplored that might be closely linked to pathological mechanisms. For this reason, it should be considered as a distinct therapeutic target with respect to cytoplasmic Tau.

Overall, our results indicate an association between Tau and the glutamatergic function, further supporting that the pathological state of Tau might be involved in glutamatergic alteration during the progression of the disease.

Experimental Procedures

Cell culture, transfections and treatments

Immortalized hippocampal neurons HT22 were cultured in Dulbecco's modified Eagle's medium (DMEM) (GIBCO) supplemented with 10% FBS. The day before the experiment cells were seeded at 10^5 cells in six-well plates or in Willco dishes (Willcowells). Transient transfection was carried out with Lipofectamine 2000 (Thermo-Fisher) according to manufacturer's instructions. The transfection efficiency was measured by YFP expression and resulted about 40%.

Mouse embryonic stem cell-derived neuronal cultures were induced and maintained as previously described.[46] In brief, embryonic stem cells from mouse blastulae were harvested at E13.5, alternatingly maintained in embryonic stem cell media + 10% fetal bovine serum comprised of GMEM BHK-21 (11710035, ThermoFisher Scientific), 2 mM Glutamine (25030, ThermoFisher Scientific), 1 mM Sodium Pyruvate (11360070, ThermoFisher Scientific), 100 U/ml Penicillin-streptomycin (15140, ThermoFisher Scientific), 1 mM Non-essential amino acids (11140, Sigma Aldrich), 0.05 mM β-mercaptoethanol (M3148, Sigma Aldrich), Mouse Leukemia Inhibitory Factor (LIF), 10 ng/ml (GFM200-100, Cell Guidance Systems), N-2 Supplement 100X (175020, ThermoFisher Scientific), and B-27 Supplement minus Vitamin A 50X (125870, ThermoFisher Scientific) and dual GSK-3b/MAPK inhibition + recombinant mouse LIF media containing GMEM BHK-21 (11710035, ThermoFisher Scientific) and containing 2 mM Glutamine (25030, ThermoFisher Scientific), 1 mM Sodium Pyruvate (11360070, ThermoFisher Scientific), 100 U/ml Penicillin-streptomycin (15140, ThermoFisher Scientific), 1 mM Non-essential amino acids (11140, Sigma Aldrich), 0.05 mM β-mercaptoethanol (M3148, Sigma Aldrich), CHIR 99201, 5 μM (SML1046, Sigma Aldrich), PD 0325901, 5 μM (sc-205427, Santa Cruz Biotechnologies), Mouse Leukemia Inhibitory Factor (LIF), 10 ng/ml (GFM200-100, Cell Guidance Systems), N-2 Supplement 100X (175020, ThermoFisher Scientific), and B-27 Supplement minus Vitamin A 50X (125870, ThermoFisher Scientific) (2i + LIF). After three cycles cells were seeded at a density of ~30,000 cells/cm^2 on 0.1% porcine gelatin (G1890, Sigma Aldrich) and briefly maintained in 2i + LIF media for 1–2 days before changing the media to neural induction containing Wnt and BMP inhibitors (WiBi), comprised of DMEM/F12 1:1 (21331-046, ThermoFisher Scientific) containing 2 mM Glutamine (25030, ThermoFisher Scientific), 1 mM Sodium Pyruvate (11360070, ThermoFisher Scientific), 100 U/ml Penicillin-streptomycin (15140, ThermoFisher Scientific), 1 mM Non-essential amino acids (11140, Sigma Aldrich), 0.05 mM β-mercaptoethanol (M3148, Sigma Aldrich), 10 μM 53AH (C5324-10, Cellagen Technology), 10 μM LDN193189 hydrochloride (SML0559, Sigma Aldrich), N-2 Supplement 100X (175020, ThermoFisher Scientific), and B-27 Supplement minus Vitamin A 50X (125870, ThermoFisher Scientific). Cells were expanded for 10 days in vitro in WiBi media, passaging the third and seventh days in vitro (DIV) onto poly-l-ornithine (P3655, Sigma Aldrich) and purified mouse laminin (CC095-M, Merck Millipore) at 40,000 and 100,000 cells/cm^2, respectively. On the eleventh day from neural induction, the media was changed to minimal basal media comprised of Neurobasal (21103049, ThermoFisher Scientific) and containing 2 mM Glutamine (25030, ThermoFisher Scientific), 1 mM Sodium Pyruvate (11360070, ThermoFisher Scientific), 100 U/ml Penicillin-streptomycin (15140,

ThermoFisher Scientific), 0.05 mM β-mercaptoethanol (M3148, Sigma Aldrich), Ascorbate, 0.5 mM (A92902, Sigma Aldrich), and B-27 Supplement minus Vitamin A 50X (125870, ThermoFisher Scientific). Cells were transfected by Lipofectamine 2000 (Thermo-Fisher) at DIV 13. Seeding experiments were performed at DIV 17 for three days and then cells were fixed. Tau-YFP-NLS construct cloning: a triplicated nuclear localization signal (NLS) was amplified from pDonor-tBFP-NLS-Neo using a forward primer incorporating BsrGI restriction site in its 5′tail (5′TGTACAAGTCCGGACTCAGATC3′) and the reverse primer 5′AACAAGTTAACAACAACAATTGCAT3′. The amplification product was first T-A cloned in pCR2.1 and then subcloned BsrGI-NotI into pEYFP, in order to obtain pEYFP-NLS. The AgeI fragment from pTauRSIVT-EYFP (encompassing pTauRSIVT)[47] was then cloned in pEYFP-NLS to obtain pTauRSIVT-EYFP-NLS. The P301S mutant has been generated by the Q5 Site-Directed Mutagenesis Kit (New England BioLabs) primer Fwd: 5′-CAAACACGTCTCGGGAGGCGG-3′; primer Rev 5′-ATATTATCCTTTGAGCCACACTTGGAC-3′.

Western blot and immunostaining

Total protein extracts were prepared in lysis buffer supplemented with protease and phosphatase inhibitors. The Subcellular Protein Fractionation Kit for Cultured Cells (Thermo-Fisher) was used according to manufacturer's instructions.[48] Proteins were quantified by BCA (Thermo-Fisher). For each sample 20 μg of each fraction were loaded. Proteins were separated by SDS-PAGE and electro-blotted onto Hybond-C-Extra (Amersham Biosciences) nitrocellulose membranes. The total extracts and the CF were loaded on a 12% acrylamide gel; instead, NF fractions were loaded on 8% acrylamide gel. Membranes were blocked (5% skimmed milk powder in TBS, 0.1% Tween 20).

For IF experiments, cells were fixed with ice-cold 100% methanol for 5 min. After permeabilization (PBS, 0.1% Triton-X100) samples were blocked (1% wt/vol BSA) and incubated with primary and secondary antibodies. Slides were mounted with Vectashield mounting medium (Vector Laboratories).

Primary antibodies for WB: mouse anti-Tau (Tau5) 1:1000 ab80579 (AbCam); rabbit anti-histone H2b (Santa Cruz); mouse anti-GAPDH 1:15000 (Fitzgerald); rabbit anti-VGluT1 ab77822 1:500 (AbCam). Secondary antibodies for Western blot analysis were HRP-conjugated anti-mouse or anti-rabbit, purchased from Santa Cruz Biotechnology, Inc., Santa Cruz, CA, USA.

Primary antibodies for IF: mouse anti-tau (Tau-13) 1:500 (Santa Cruz); rabbit anti-VGluT1 ab77822 1:500 (AbCam). Secondary antibodies for IF: Alexa Fluor 633; Alexa Fluor 488 (Life Technologies). For K114 staining, cells were fixed and permeabilized as described above. Samples were incubated with 1 μM K114 (Sigma-Aldrich) for 10 min and slides were mounted with VECTASHIELD. Nuclear staining performed by incubation for 15 min with TOTO-3 or NuclearID. Western blot quantification has been performed using ImageJ software.

Real-time PCR

Total RNA was extracted by Nucleospin (Macherey-Nagel) and retro-transcribed by Reverse Transcriptase Core kit (Eurogentec) according to manufacturer's instructions. Real-time PCR was performed using the iTaqTM Universal SYBR® Green Supermix (BioRad), and performed for 40 cycles of amplification with denaturation at 95 °C for 15 s, annealing at 60 °C for 25 s, extension at 72 °C for 20 s. The primers employed were: Actin: fwd 5′-TCCATCCTGGCCTCACTGTCCAC-3′, rev 5′-GAGGGGCCGGACTCATCGTACT-3′; Tau: fwd 5′-GTGACCTCCAAGTGTGGCTCATT-3′, rev 5′-CTTCGACTGGACTCTGTCCTTG-3′; VGluT1: fwd 5′-GAGGAGTGGCAGTACGTGTTCC-3′, rev 5′-TCTCCAGAAGCAAAGACCCC-3′.

Tau seeding

Recombinant heparin-assembled P301S Tau fibrils were prepared as previously described.[30] Cells were plated in glass bottom dishes as previously described and 1.2 μg of P301S Tau fibrils were delivered to cells with 2 μl of Lipofectamine 2000 transfection reagent diluted in 300 μl of Opti-MEM Reduced Serum Medium (Gibco). Cells were treated for 2 h, then DMEM low glucose was added.

Image acquisition and analysis

A Leica TCS SP8 confocal laser-scanning microscope (Leica Microsystems, Mannheim, Germany) equipped with Leica Application Suite (LAS) X software was used. All frames were captured by means of HC PL APO CS2 40X/1.30 (*) oil objective, a format size of 512 × 512 pixel and a sequential scan procedure. All confocal frames were taken by a suitable scanning power and speed along with gain level to achieve the greater signal definition and avoid any background noise. (*) N.A. = 1.30. A heated and humidified chamber mounted on the stage of the microscope was used for live imaging experiments in order to maintain a controlled temperature (37 °C) and CO2 (5%) during image acquisition. An Argon laser was used for ECFP (λ = 458 nm) and EYFP (λ = 514 nm), a Gre-Ne laser for NuclearID (λ = 543 nm) and a He-Ne laser for TOTO-3 (λ = 633 nm). The UV laser was used for K114 (λ = 380 nm).

GSEA

The transcriptome of the prefrontal cortex of AD patients was derived from the GSE84422 dataset Affymetrix HG-U133A microarray platform.[31] The prefrontal cortex dataset includes 7 patients at Braak stage 1, 8 patients at Braak stage 2, 13 patients at Braak stage 3, 11 patients at Braak stage 4, 16 patients at Braak stage 6. No stage 5 patients are present. Samples were filtered by brain region with R package simpleaffy[49] and the log2-transformed expression of VGluT1 was plotted as a function of the Braak stage. Two probes to measure VGluT1 expression are available: 204229_at, 204230_s_at. For each patient the median of the two probes has been reported. P-values were computed by Kruskal-Wallis ANOVA. For GSEA, differential gene expression in the prefrontal cortex at each stage was calculated with R package limma,[50] probes were ranked by log2 fold change and GSEA was performed using WebGestalt[51] with the standard settings and with affy_hg_u133a as the reference set. KEGG pathways with FDR < 0.05 were deemed statistically significant.

Statistical analysis

For Western Blot and quantitative real-time PCR, statistical significance was assessed by non-parametric Kruskal-Wallis test followed by pairwise Mann-Whitney test (one tailed). For qPCR, gene expression was calculated with Pfaffl method.[52] Each sample was run in triplicate and at least four biological replicates were performed for each experiment. All results are shown as mean ± SEM from at least four independent experiments. For fluorescence image analysis ANOVA coupled with Tukey's *t*-test has been used. Significance is indicated as * for $p < 0.05$, ** for $p < 0.01$, *** for $p < 0.001$ and **** for $p < 0.0001$.

Author Contributions

GS, CDP and AC designed experimentation and wrote the manuscript. GS, MV, AS, KD, LP, MCC and CDP performed the experiments; GS, MV and AS collected and analysed the data. FC, AC and MC provided reagents and contributed with discussion and correction of the manuscript.

Acknowledgments

Declaration of Interests

The authors declare that the research was conducted in the absence of any commercial or financial relationships that could be construed as a potential conflict of interest.

Appendix A. Supplementary material

Supplementary data to this article can be found online at https://doi.org/10.1016/j.jmb.2020.10.009.

† Present address: Genome Biology Unit, European Molecular Biology Laboratory (EMBL), Heidelberg, Germany.
‡ Present address: Oxford Parkinson's Disease Center, Department of Physiology, Anatomy and Genetics, University of Oxford, Oxford, United Kingdom.

References

1. Lane, C.A., Hardy, J., Schott, J.M., (2018). Alzheimer's disease. *Eur. J. Neurol.*, **25**, 59–70. https://doi.org/10.1111/ene.13439.

2. Iqbal, K., Liu, F., Gong, C.-X., Grundke-Iqbal, I., (2010). Tau in Alzheimer disease and related tauopathies. *Curr. Alzheimer Res.*, **7**, 656–664. https://doi.org/10.2174/156720510793611592.

3. Deture, M.A., Dickson, D.W., (2019). The neuropathological diagnosis of Alzheimer's disease. *Mol. Neurodegener.*, **14**, 1–18. https://doi.org/10.1186/s13024-019-0333-5.

4. Bakota, L., Brandt, R., (2016). Tau biology and tau-directed therapies for Alzheimer's disease. *Drugs*, **76**, 301–313. https://doi.org/10.1007/s40265-015-0529-0.

5. Miller, S.L., Fenstermacher, E., Bates, J., Blacker, D., Sperling, R.A., Dickerson, B.C., (2008). Hippocampal activation in adults with mild cognitive impairment predicts subsequent cognitive decline. *J. Neurol. Neurosurg. Psych.*, **79**, 630–635. https://doi.org/10.1136/jnnp.2007.124149.

6. Kazim, S.F., Chuang, S.C., Zhao, W., Wong, R.K.S., Bianchi, R., Iqbal, K., (2017). Early-onset network hyperexcitability in presymptomatic Alzheimer's disease transgenic mice is suppressed by passive immunization with anti-human APP/Aβ antibody and by mGluR5 blockade. *Front. Aging Neurosci.*, **9**, 1–17. https://doi.org/10.3389/fnagi.2017.00071.

7. Bell, K.F.S., Bennett, D.A., Cuello, A.C., (2007). Paradoxical upregulation of glutamatergic presynaptic boutons during mild cognitive impairment. *J. Neurosci.*, **27**, 10810–10817. https://doi.org/10.1523/JNEUROSCI.3269-07.2007.

8. Pasquini, L., Rahmani, F., Maleki-Balajoo, S., La Joie, R., Zarei, M., Sorg, C., Drzezga, A., Tahmasian, M., (2019). Medial temporal lobe disconnection and hyperexcitability across Alzheimer's disease stages. *J. Alzheimer's Dis. Reports*, **3**, 103–112. https://doi.org/10.3233/adr-190121.

9. Findley, C.A., Bartke, A., Hascup, K.N., Hascup, E.R., (2019). Amyloid beta-related alterations to glutamate signaling dynamics during alzheimer's disease progression. *ASN Neuro*, **11** https://doi.org/10.1177/1759091419855541.

10. Wang, R., Reddy, P.H., (2017). Role of glutamate and NMDA receptors in Alzheimer's disease. *J. Alzheimer's Dis.*, **57**, 1041–1048. https://doi.org/10.3233/JAD-160763.

11. Esposito, Z., Belli, L., Toniolo, S., Sancesario, G., Bianconi, C., Martorana, A., (2013). Amyloid β, glutamate, excitotoxicity in Alzheimer's disease: are we on the right track?. *CNS Neurosci. Ther.*, **19**, 549–555. https://doi.org/10.1111/cns.12095.

12. Wu, J.W., Hussaini, S.A., Bastille, I.M., Rodriguez, G.A., Mrejeru, A., Rilett, K., Sanders, D.W., Cook, C., et al., (2016). Neuronal activity enhances tau propagation and tau pathology in vivo. *Nature Neurosci.*, **19**, 1085–1092. https://doi.org/10.1038/nn.4328.

13. Kirvell, S.L., Esiri, M., Francis, P.T., (2006). Down-regulation of vesicular glutamate transporters precedes cell loss and pathology in Alzheimer's disease. *J. Neurochem.*, **98**, 939–950. https://doi.org/10.1111/j.1471-4159.2006.03935.x.

14. Stancu, I.C., Vasconcelos, B., Ris, L., Wang, P., Villers, A., Peeraer, E., Buist, A., Terwel, D., et al., (2015). Templated misfolding of Tau by prion-like seeding along neuronal connections impairs neuronal network function and associated behavioral outcomes in Tau transgenic mice. *Acta Neuropathol.*, **129**, 875–894. https://doi.org/10.1007/s00401-015-1413-4.

15. Decker, J.M., Krüger, L., Sydow, A., Zhao, S., Frotscher, M., Mandelkow, E., Mandelkow, E.M., (2015). Pro-aggregant Tau impairs mossy fiber plasticity due to structural changes and Ca(++) dysregulation. *Acta Neuropathol. Commun.*, **3**, 23. https://doi.org/10.1186/s40478-015-0193-3.

16. Avila, J., Llorens-Martín, M., Pallas-Bazarra, N., Bolós, M., Perea, J.R., Rodríguez-Matellán, A., Hernández, F., (2017). Cognitive decline in neuronal aging and Alzheimer's disease: Role of NMDA receptors and associated proteins. *Front. Neurosci.*, **11**, 1–9. https://doi.org/10.3389/fnins.2017.00626.

17. Lau, D.H.W., Hogseth, M., Phillips, E.C., O'Neill, M.J., Pooler, A.M., Noble, W., Hanger, D.P., (2016). Critical residues involved in tau binding to fyn: implications for tau phosphorylation in Alzheimer's disease. *Acta Neuropathol. Commun.*, **4**, 49. https://doi.org/10.1186/s40478-016-0317-4.

18. Li, C., Götz, J., (2017). Somatodendritic accumulation of Tau in Alzheimer's disease is promoted by Fyn-mediated local protein translation. *EMBO J.*, **36**, 3120–3138. https://doi.org/10.15252/embj.201797724.

19. Mondragón-Rodríguez, S., Trillaud-Doppia, E., Dudilot, A., Bourgeois, C., Lauzon, M., Leclerc, N., Boehm, J., (2012). Interaction of endogenous tau protein with synaptic proteins is regulated by N-methyl-D-aspartate receptor-dependent tau phosphorylation. *J. Biol. Chem.*, **287**, 32040–32053. https://doi.org/10.1074/jbc.M112.401240.

20. Hall, A.M., Throesch, B.T., Buckingham, S.C., Markwardt, S.J., Peng, Y., Wang, Q., Hoffman, D.A., Roberson, E.D., (2015). Tau-dependent Kv4.2 depletion and dendritic hyperexcitability in a mouse model of Alzheimer's disease. *J. Neurosci.*, **35**, 6221–6230. https://doi.org/10.1523/JNEUROSCI.2552-14.2015.

21. Khadrawyb, E.H., (2014). Glutamate excitotoxicity and neurodegeneration. *J. Mol. Genet. Med.*, **8**, 8–11. https://doi.org/10.4172/1747-0862.1000141.

22. Sánchez, M.P., García-Cabrero, A.M., Sánchez-Elexpuru, G., Burgos, D.F., Serratosa, J.M., (2018). Tau-induced pathology in epilepsy and dementia: Notions from patients and animal models. *Int. J. Mol. Sci.*, **19** https://doi.org/10.3390/ijms19041092.

23. Holth, J.K., Bomben, V.C., Reed, J.G., Inoue, T., Younkin, L., Younkin, S.G., Pautler, R.G., Botas, J., et al., (2013). Tau loss attenuates neuronal network hyperexcitability in mouse and Drosophila genetic models of epilepsy. *J. Neurosci.*, **33**, 1651–1659. https://doi.org/10.1523/JNEUROSCI.3191-12.2013.

24. DeVos, S.L., Goncharoff, D.K., Chen, G., Kebodeaux, C.S., Yamada, K., Stewart, F.R., Schuler, D.R., Maloney, S.E., et al., (2013). Antisense reduction of tau in adult mice protects against seizures. *J. Neurosci.*, **33**, 12887–12897. https://doi.org/10.1523/JNEUROSCI.2107-13.2013.

25. Delacourte, A., David, J.P., Sergeant, N., Buée, L., Wattez, A., Vermersch, P., Ghozali, F., Fallet-Bianco, C., et al., (1999). The biochemical pathway of neurofibrillary degeneration in aging and Alzheimer's disease. *Neurology.*, **52**, 1158–1165. https://doi.org/10.1212/wnl.52.6.1158.

26. Alonso, A.D.C., Li, B., Grundke-Iqbal, I., Iqbal, K., (2008). Mechanism of tau-induced neurodegeneration in Alzheimer disease and related tauopathies. *Curr. Alzheimer Res.*, **5**, 375–384. https://doi.org/10.2174/156720508785132307.

27. Jadhav, S., Cubinkova, V., Zimova, I., Brezovakova, V., Madari, A., Cigankova, V., Zilka, N., (2015). Tau-mediated synaptic damage in Alzheimer's disease. *Transl. Neurosci.*, **6**, 214–226. https://doi.org/10.1515/tnsci-2015-0023.

28. Guo, T., Noble, W., Hanger, D.P., (2017). Roles of tau protein in health and disease. *Acta Neuropathol.*, **133**, 665–704. https://doi.org/10.1007/s00401-017-1707-9.

29. Siano, G., Varisco, M., Caiazza, M.C., Quercioli, V., Mainardi, M., Ippolito, C., Cattaneo, A., Di Primio, C., (2019). Tau modulates VGluT1 expression. *J. Mol. Biol.*, **431**, 873–884. https://doi.org/10.1016/j.jmb.2019.01.023.

30. Siano, G., Caiazza, M.C., Ollà, I., Varisco, M., Madaro, G., Quercioli, V., Calvello, M., Cattaneo, A., et al., (2019). Identification of an ERK inhibitor as a therapeutic drug against tau aggregation in a new cell-based assay. *Front. Cell. Neurosci.*, **13**, 386. https://doi.org/10.3389/fncel.2019.00386.

31. Wang, M., Roussos, P., McKenzie, A., Zhou, X., Kajiwara, Y., Brennand, K.J., De Luca, G.C., Crary, J.F., et al., (2016). Integrative network analysis of nineteen brain regions identifies molecular signatures and networks underlying selective regional vulnerability to Alzheimer's disease. *Genome Med.*, **8**, 104. https://doi.org/10.1186/s13073-016-0355-3.

32. Kashani, A., Lepicard, E., Poirel, O., Videau, C., David, J.P., Fallet-Bianco, C., Simon, A., Delacourte, A., et al., (2008). Loss of VGLUT1 and VGLUT2 in the prefrontal cortex is correlated with cognitive decline in Alzheimer

disease. *Neurobiol. Aging.*, **29**, 1619–1630. https://doi.org/10.1016/j.neurobiolaging.2007.04.010.

33. Revett, T.J., Baker, G.B., Jhamandas, J., Kar, S., (2013). Glutamate system, amyloid β peptides and tau protein: functional interrelationships and relevance to Alzheimer disease pathology. *J. Psychiatry Neurosci.*, **38**, 6–23. https://doi.org/10.1503/jpn.110190.

34. Hoshi, A., Tsunoda, A., Yamamoto, T., Tada, M., Kakita, A., Ugawa, Y., (2018). Altered expression of glutamate transporter-1 and water channel protein aquaporin-4 in human temporal cortex with Alzheimer's disease. *Neuropathol. Appl. Neurobiol.*,.

35. Crescenzi, R., DeBrosse, C., Nanga, R.P.R., Byrne, M.D., Krishnamoorthy, G., D'Aquilla, K., Nath, H., Morales, K.H., et al., (2017). Longitudinal imaging reveals sub-hippocampal dynamics in glutamate levels associated with histopathologic events in a mouse model of tauopathy and healthy mice. *Hippocampus.*, **27**, 285–302. https://doi.org/10.1002/hipo.22693.

36. Metuzals, J., Robitaille, Y., Houghton, S., Gauthier, S., Leblanc, R., (1988). Paired helical filaments and the cytoplasmic-nuclear interface in Alzheimer's disease. *J. Neurocytol.*, **17**, 827–833. https://doi.org/10.1007/BF01216709.

37. Fernández-Nogales, M., Cabrera, J.R., Santos-Galindo, M., Hoozemans, J.J.M., Ferrer, I., Rozemuller, A.J.M., Hernández, F., Avila, J., et al., (2014). Huntington's disease is a four-repeat tauopathy with tau nuclear rods. *Nature Med.*, **20**, 881–885. https://doi.org/10.1038/nm.3617.

38. Benhelli-Mokrani, H., Mansuroglu, Z., Chauderlier, A., Albaud, B., Gentien, D., Sommer, S., Schirmer, C., Laqueuvre, L., et al., (2018). Genome-wide identification of genic and intergenic neuronal DNA regions bound by Tau protein under physiological and stress conditions. *Nucleic Acids Res.*, **1**, 1–18. https://doi.org/10.1093/nar/gky929.

39. Sanders, D.W., Kaufman, S.K., DeVos, S.L., Sharma, A.M., Mirbaha, H., Li, A., Barker, S.J., Foley, A.C., et al., (2014). Distinct tau prion strains propagate in cells and mice and define different tauopathies. *Neuron*, **82**, 1271–1288. https://doi.org/10.1016/j.neuron.2014.04.047.

40. Yoshiyama, Y., Higuchi, M., Zhang, B., Huang, S.-M., Iwata, N., Saido, T.C., Maeda, J., Suhara, T., et al., (2007). Synapse loss and microglial activation precede tangles in a P301S tauopathy mouse model. *Neuron*, **53**, 337–351. https://doi.org/10.1016/j.neuron.2007.01.010.

41. Lewis, J., McGowan, E., Rockwood, J., Melrose, H., Nacharaju, P., Van Slegtenhorst, M., Gwinn-Hardy, K., Paul Murphy, M., et al., (2000). Neurofibrillary tangles, amyotrophy and progressive motor disturbance in mice

expressing mutant (P301L) tau protein. *Nat. Genet.*, **25**, 402–405. https://doi.org/10.1038/78078.

42. Braak, H., Del Tredici, K., (2018). Spreading of tau pathology in sporadic Alzheimer's disease along cortico-cortical top-down connections. *Cereb. Cortex*, **28**, 3372–3384. https://doi.org/10.1093/cercor/bhy152.

43. Lowe, V.J., Wiste, H.J., Senjem, M.L., Weigand, S.D., Therneau, T.M., Boeve, B.F., Josephs, K.A., Fang, P., et al., (2018). Widespread brain tau and its association with ageing, Braak stage and Alzheimer's dementia. *Brain.*, **141**, 271–287. https://doi.org/10.1093/brain/awx320.

44. Sampath, D., Sathyanesan, M., Newton, S.S., (2017). Cognitive dysfunction in major depression and Alzheimer's disease is associated with hippocampal–prefrontal cortex dysconnectivity. *Neuropsychiatr. Dis. Treat.*, **13**, 1509–1519. https://doi.org/10.2147/NDT.S136122.

45. van Marum, R.J., (2009). Update on the use of memantine in Alzheimer's disease. *Neuropsychiatr. Dis. Treat.*, **5**, 237–247. https://doi.org/10.2147/ndt.s4048.

46. Bertacchi, M., Pandolfini, L., Murenu, E., Viegi, A., Capsoni, S., Cellerino, A., Messina, A., Casarosa, S., et al., (2013). The positional identity of mouse ES cell-generated neurons is affected by BMP signaling. *Cell. Mol. Life Sci.*, **70**, 1095–1111. https://doi.org/10.1007/s00018-012-1182-3.

47. Di Primio, C., Quercioli, V., Siano, G., Rovere, M., Kovacech, B., Novak, M., Cattaneo, A., (2017). The distance between N and C termini of tau and of FTDP-17 mutants is modulated by microtubule interactions in living cells. *Front. Mol. Neurosci.*, **10**, 1–13. https://doi.org/10.3389/fnmol.2017.00210.

48. Siano, G., Caiazza, M.C., Varisco, M., Calvello, M., Quercioli, V., Cattaneo, A., Di Primio, C., (2019). Modulation of tau subcellular localization as a tool to investigate the expression of disease-related genes. *J. Vis. Exp.*,. https://doi.org/10.3791/59988.

49. Miller, C. (2020). simpleaffy: Very simple high level analysis of Affymetrix data. https://doi.org/10.18129/B9.bioc.simpleaffy.

50. Ritchie, M.E., Phipson, B., Wu, D., Hu, Y., Law, C.W., Shi, W., Smyth, G.K., (2015). limma powers differential expression analyses for RNA-sequencing and microarray studies e47–e47 *Nucleic Acids Res.*, **43** https://doi.org/10.1093/nar/gkv007.

51. Liao, Y., Wang, J., Jaehnig, E.J., Shi, Z., Zhang, B., WebGestalt, (2019). gene set analysis toolkit with revamped UIs and APIs. *Nucleic Acids Res.*, **47**, W199–W205. https://doi.org/10.1093/nar/gkz401.

52. Pfaffl, M.W., (2001). A new mathematical model for relative quantification in real-time RT-PCR 45e–45e *Nucleic Acids Res.*, **29** https://doi.org/10.1093/nar/29.9.e45.